

# $^{119}\text{Sn}$ Mössbauer studies on ferromagnetic and photocatalytic Sn–TiO<sub>2</sub> nanocrystals

Ayyakannu Sundaram Ganeshraja<sup>1</sup> · Kiyoshi Nomura<sup>2</sup> · Junhu Wang<sup>1</sup>

© Springer International Publishing Switzerland 2016

**Abstract** Diluted Sn doped TiO<sub>2</sub> nanocrystals (Sn/Ti ratio:  $x \leq 1.37\%$ ) were synthesized by a simple hydrothermal method using pure reagents without any surfactant and dispersant material. The XRD of these samples showed an anatase phase, anatase and rutile mixed phases, and a rutile phase of TiO<sub>2</sub> and SnO<sub>2</sub> with the increase of Sn dopant concentrations.  $^{119}\text{Sn}$  Mössbauer spectra gave the broad peaks, which were decomposed into doublets and sextets because almost all these samples showed magnetic hysteresis even at room temperature. The titanium oxides doped with  $x \leq 0.12\%$  showed the relatively large magnetic hysteresis and high photocatalytic activity. Mössbauer spectra of samples doped with  $x > 0.3\%$  were analyzed by one doublet and two sextets although the samples showed weak ferromagnetism. Three kinds of Sn species may be distinguished as Sn<sup>4+</sup> substituted TiO<sub>2</sub> and two different magnetic arrangements of Sn doped TiO<sub>2</sub>: one with more oxygen defects and other at the interface of TiO<sub>2</sub> and precipitated SnO<sub>2</sub> containing Ti atoms. The correlation between various amounts of Sn sites and photocatalytic activity and/or magnetic property was discussed.

**Keywords** Sn-TiO<sub>2</sub> ·  $^{119}\text{Sn}$  Mössbauer study · Ferromagnetic · Photocatalyst · Rhodamine B

---

This article is part of the Topical Collection on *Proceedings of the 2nd Mediterranean Conference on the Applications of the Mössbauer Effect (MECAME 2016), Cavtat, Croatia, 31 May–3 June 2016*

---

✉ Junhu Wang  
wangjh@dicp.ac.cn

<sup>1</sup> Mössbauer Effect Data Center, Dalian Institute of Chemical Physics, Chinese Academy of Science, Dalian 116023, China

<sup>2</sup> Photocatalysis International Research Center, Tokyo University of Science, Yamazaki, Noda, Ciba 278-8510, Japan

## 1 Introduction

A tin doped titanium dioxide (Sn–TiO<sub>2</sub>) nanocomposite has received attention as a good photocatalyst for the remediation of organic pollutants and the photogeneration of hydrogen from water [1–3]. The Sn–TiO<sub>2</sub> nanocomposite has high photocatalytic activity under visible light owing to a band gap narrowing. Li et al. [4] showed that Sn<sup>4+</sup> ions can be incorporated linearly into TiO<sub>2</sub> lattices, accompanied by a phase transformation from anatase to rutile depending on the amount of the Sn dopant. Obviously, the Sn<sup>4+</sup> doped TiO<sub>2</sub> nanoparticles display considerable structural complexity. Thus, it is difficult to understand the location and role of the Sn<sup>4+</sup> ions in the TiO<sub>2</sub> matrix. However, until now, there has been little reported on the structural and magnetic properties of Sn–TiO<sub>2</sub> by <sup>119</sup>Sn Mössbauer studies [5].

In our previous paper [6], Sn–TiO<sub>2</sub> nanocrystals were synthesized by the simple hydrothermal method. Moreover, this conventional technique was performed to obtain the formation of the anatase, anatase-rutile mixed, and rutile phases for small to high levels of tin doping. In the present work, in order to make it clear, we studied the relationship between interesting photocatalytic activity, structural and magnetic results by <sup>119</sup>Sn Mössbauer spectroscopy.

## 2 Experimental

### 2.1 Chemicals and instrumentation

Rhodamine B (RhB) was purchased from Aladdin chemicals (China). The details of all other chemicals were given in our previous report [6]. All the chemicals with at least analytical grade and deionised water were used for the preparation of solution samples, and the precipitated samples were dried at room temperature.

The preparation and structural characterization of present samples were reported in our previous paper [6]. The Sn–TiO<sub>2</sub> samples were denoted as Sn–Ti-x (x represents the atom ratio % of Sn/Ti, x = 0–1.37). The low level Sn doped samples are defined as x ≤ 0.30, and the high level Sn doped samples as x > 0.30. Nanoparticles with a diameter of 6–15 nm were observed in all samples.

<sup>119</sup>Sn Mössbauer spectra were collected on a Topologic 500A system at room temperature. Ca<sup>119m</sup>SnO<sub>3</sub> source was moved in a constant acceleration mode. The velocity scale was calibrated with the magnetic sextet spectrum of a high-purity  $\alpha$ -iron foil absorber and <sup>57</sup>Co(Rh) as the  $\gamma$ -ray source. The isomer shifts were given relative to CaSnO<sub>3</sub> used as the standard reference. All spectra were fitted to Lorentzian profiles by the least-squares method, and the fit quality was controlled by the standard  $\chi^2$  and misfit tests (MossWinn program). The spectrophotometric measurements were carried out on a GBC Cintra UV-vis spectrophotometer.

### 2.2 Photocatalytic activity

The photocatalytic activities of the samples were evaluated by photodegradation of RhB (10<sup>-5</sup> M) using xenon illumination system (PEILC CERMAX model LX 175/300), attached with power supply (10 A: CX-04E) and with a 420 nm long-pass filter used as the light source. The distance between the lamp and the solution was 8.0 cm.

All of the experiments were performed in a dark box. In a general photocatalytic experiment, 30 mg catalyst was dispersed in an 80 mL RhB aqueous solution in a 100 mL glass beaker at room temperature and neutral pH conditions. Then the suspension was magnetically stirred for 30 min to reach the adsorption–desorption equilibrium. Furthermore, prior to irradiation, the mixture solution was continuously stirred by a magnetic stirrer for complete mixing. 3 mL aliquots were periodically taken out from the suspension to centrifuge (15,000 rpm, 2 min) every 60 min during the evaluation process. The supernatants were measured by the instrument (GBC Cintra) to record the changes of absorption values at the wavelength of 554 nm relative to the initial RhB aqueous solutions. The photodegradation efficiencies (PDE) were calculated via the formula  $PDE = \{(A_0 - A_t)/A_0\} \times 100 \%$ , where  $A_0$  is the absorbance of initial RhB solution and  $A_t$  is the absorbance of RhB solution measured at various irradiation time at 554 nm. In order to diminish the experimental error, the experiments were repeated at least three times for the same sample and noted the mean value.

### 3 Results and discussion

The Sn–Ti- $x$  samples were prepared by simple hydrothermal and calcination processes in line with our recent article, which also outlined the structural, morphology, physicochemical and photocatalytic properties of Sn–Ti- $x$  samples [6]. The catalytic properties studied include (i) the formation of anatase, mixed anatase-rutile, and rutile phases with increasing Sn level in Sn-doped TiO<sub>2</sub>, (ii) the enhanced light absorption property in the visible region, (iii) Sn content in TiO<sub>2</sub> assisted magnetic characters and (iv) photocatalytic activities showing structural, luminescent and ferromagnetic dependences [6].

Herein, we focused on the studies on the structural and magnetic characters of Sn–Ti- $x$  samples by room temperature <sup>119</sup>Sn Mössbauer spectroscopy. Figure 1 presents the <sup>119</sup>Sn Mössbauer spectra of the Sn–Ti- $x$  samples at room temperature. Mössbauer spectra of low level Sn doped TiO<sub>2</sub> samples were decomposed into a doublet and a sextet and Mössbauer spectra of high level Sn doped samples into one more component magnetic sextet because almost all samples showed the weak ferromagnetism. The obtained <sup>119</sup>Sn Mössbauer parameters are given in Table 1. We obtained interesting inner magnetic fields of around 3T from <sup>119</sup>Sn Mössbauer spectra of low Sn doped TiO<sub>2</sub>. The doublet and magnetic sextet are considered due to paramagnetic Sn doped TiO<sub>2</sub> and defect induced magnetism, respectively. It is reasonable that all isomer shift values near the 0.0 mm/s show the valence states of Sn<sup>4+</sup> because Ti has also valence state of 4+. The ionic radius of Sn<sup>4+</sup> (69 pm) is larger than that of Ti<sup>4+</sup> (53 pm). The high Sn doped samples showed the more broadened Mössbauer spectra. We decomposed them by adding one more magnetic sextet component. The XRD and transmission electron microscope data of the highly Sn doped TiO<sub>2</sub> samples showed the rutile structure of TiO<sub>2</sub> and the trace level of rutile SnO<sub>2</sub> [6]. More complex structure of the powder grains was observed, which may be due to different configurations of Sn(Ti)O<sub>2</sub> with structural defect sites or with 2Ti atoms substituted at 2Sn atom sites. More precisely, isomer shift (IS) are found to be positive values (Table 1), which are consistent with the values reported for the Sn<sup>4+</sup> dopant in transition metal oxides [7, 8]. This fact thus suggests the occurrence of Ti–O–Sn–O–Ti chain fragments in the lattice and, consequently, insertion of dopants into the matrix [8]. The doublet having large IS and quadrupole splitting (QS) is associated with defects and vacancies that are stabilized by doping of Sn<sup>4+</sup> in TiO<sub>2</sub> lattice. However, the IS value of the sample with  $x = 1.37$  is rather small, which may show the partial product of precipitated nano SnO<sub>2</sub>.

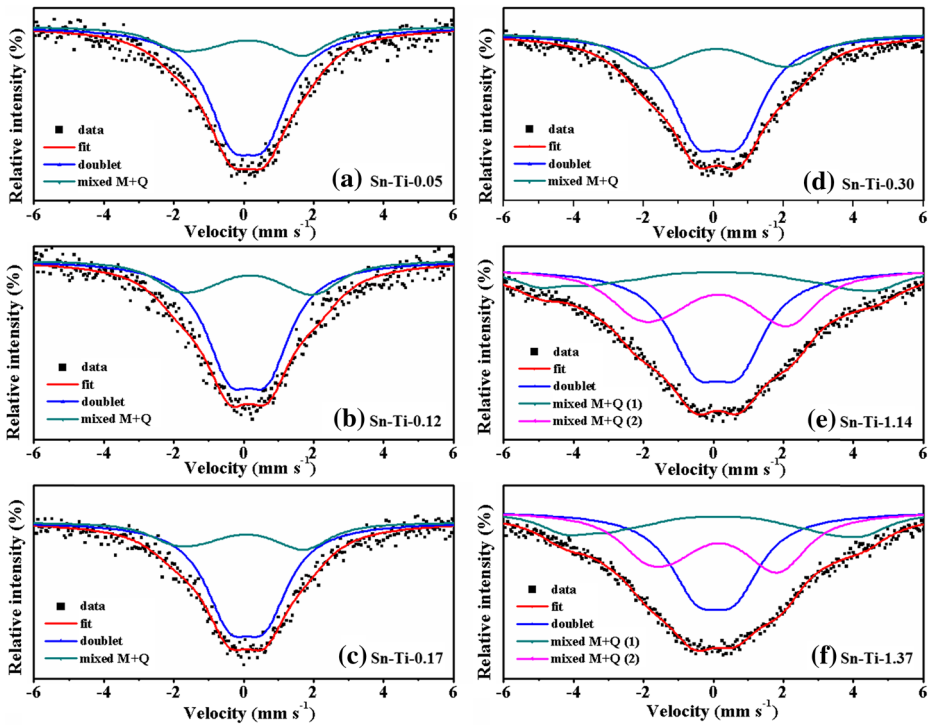


**Fig. 1** Room temperature  $^{119}\text{Sn}$  Mössbauer spectra of Sn/Ti-x(%) samples

The ferromagnetic property of the material may be initiated with the help of oxygen vacancies or structural defect sites. The oxygen vacancies present in the samples were identified from the photoluminescence spectroscopy. A strong green emission was observed at 560 nm (2.22 eV) as presented in our previous article [6]. Therefore, emissions likely originated from surface defects, such as ionizable oxygen vacancies and the recombination of self-trapped excitons (STEs) which are localized within  $\text{TiO}_6$  octahedra. The formation of oxygen vacancies were confirmed from EPR measurement for Sn-Ti-0.12 sample in our previous study [5]. However, the doublets of Sn-Ti-x samples have high QS values compared with pure  $\text{SnO}_2$ . This high QS value is due to the formation of oxygen vacancies or structural defects as a consequence of the presence of incorporated  $\text{Ti}^{4+}$ . These may be the main source of induced magnetism. Therefore, we may expect magnetically split component in the samples.

Hence, the broad peaks are assumed to consist of one doublet and two magnetic sextet components. The broad sextets may come from the magnetic relaxation of spin-lattice interaction. It is considered to be important for the induced magnetism that  $\text{Sn}^{4+}$  ions are embedded into  $\text{TiO}_2$  matrix as much as possible and do not segregate as diamagnetic  $\text{SnO}_2$  except  $x = 1.14$  and 1.37. However, the samples with  $x = 1.14$  and 1.37 showed the rutile structures mixed with  $\text{TiO}_2$  incorporated with dilute Sn and the precipitated  $\text{SnO}_2$  incorporated with dilute Ti [6, 9]. The magnetic fields of sextet 1 and sextet 2 in Sn-Ti-1.14 and Sn-Ti-1.37 samples may have different structural and electronic spin arrangements. As each

**Table 1** Mössbauer parameters (isomer shift (IS), quadrupole splitting (QS), line width (LW), chi-square ( $\chi^2$ ) and relative area intensity) of Sn-Ti-x samples at room temperature

Sample	Sn-Ti-0.05	Sn-Ti-0.12	Sn-Ti-0.17	Sn-Ti-0.30	Sn-Ti-1.14	Sn-Ti-1.37
$\chi^2$	575.88	589.22	573.05	623.18	669.48	692.40
Normalized $\chi^2$	1.14	1.17	1.14	1.24	1.34	1.39
Doublet	74.8 %	71.0 %	73.4 %	69.1 %	46.7 %	40.5 %
IS (mm s <sup>-1</sup> )	0.12 (0.02)	0.13 (0.02)	0.09 (0.01)	0.13 (0.01)	0.12 (0.01)	0.06 (0.01)
QS (mm s <sup>-1</sup> )	0.99 (0.07)	1.09 (0.05)	1.03 (0.04)	1.20 (0.03)	1.22 (0.03)	1.09 (0.04)
LW (mm s <sup>-1</sup> )	1.65	1.65	1.65	1.79	1.86	1.86
Mixed M+Q (1)	–	–	–	–	17.8 %	21.7 %
IS (mm s <sup>-1</sup> )	–	–	–	–	0.01 (0.07)	0.09 (0.04)
Magnetic field (T)	–	–	–	–	7.28 (0.13)	6.40 (0.12)
QS (mm s <sup>-1</sup> )	–	–	–	–	–0.24 (0.08)	–0.12 (0.07)
LW (mm s <sup>-1</sup> )	–	–	–	–	1.86	1.86
Mixed M+Q (2)	25.2 %	29.0 %	26.6 %	30.9 %	35.5 %	37.8 %
IS (mm s <sup>-1</sup> )	0.04 (0.08)	0.16 (0.06)	0.01 (0.05)	0.11 (0.03)	0.11 (0.02)	0.12 (0.02)
Magnetic field (T)	2.89 (0.27)	3.13 (0.18)	2.98 (0.15)	3.38 (0.09)	3.46 (0.06)	3.01 (0.07)
QS (mm s <sup>-1</sup> )	–0.25 (0.26)	–0.08(0.18)	–0.19(0.16)	0.08 (0.09)	–0.12(0.05)	–0.17(0.05)
LW (mm s <sup>-1</sup> )	1.65	1.65	1.65	1.79	1.86	1.86

has different fields, these may show ferrimagnetic behavior by creating different defect configurations. The above explanation may be reasonable that the magnetizations of Sn-Ti-1.14 and Sn-Ti-1.37 samples were weaker than that of the other three samples.

The photocatalytic activities of the obtained Sn-Ti-x samples were measured using the degradation of RhB aqueous solution under visible light irradiation ( $\geq 420$  nm). For comparison, the photocatalytic activity of undoped TiO<sub>2</sub> (anatase) nanoparticles was also measured under the similar conditions. Obviously, the undoped anatase TiO<sub>2</sub> showed the lower degradation of RhB under visible-light illumination. This involves the excitation of color dye under visible light irradiation, injection of electron from dye to TiO<sub>2</sub>, and then surface reaction, with the electron back-injection as the side process [10]. Figure 2a shows the PDE of RhB versus irradiation time. The low level Sn doped samples shows clearly higher efficiencies (~96 %) in the photocatalytic degradation of RhB than the high level Sn doped and undoped samples (for t = 120 min). It is considered that high level of Sn doping induced likely the recombination of photogenerated electrons and holes, resulting in the decrease of photocatalytic activity of TiO<sub>2</sub> [11]. This behavior is due to the phase transformation of the crystals as the dopant content is enhanced. In general, the photocatalytic performance of an anatase phase is considered superior to that of the more stable rutile phase of titania. This is attributed to the fact that anatase is very effective in photocatalytic activity due to the higher density of localized electronic states, the existence of surface-adsorbed hydroxyl species and the slower recombination of electron and hole in the crystals. From powder X-ray diffraction measurement, the pure anatase (Sn-Ti-0.05 and Sn-Ti-0.12), predominant anatase and minute rutile phases (Sn-Ti-0.17), equal portion of anatase and rutile (Sn-Ti-0.30) and pure rutile (Sn-Ti-1.14 and Sn-Ti-1.37) phases were reported in our previous paper [6]. In this case pure anatase phase and predominant anatase and small rutile phases are showing very good photocatalytic activity, while equal portion of anatase and rutile phase (Sn-Ti-0.30) sample is showing poor photocatalytic activity than that of other phases prepared in this

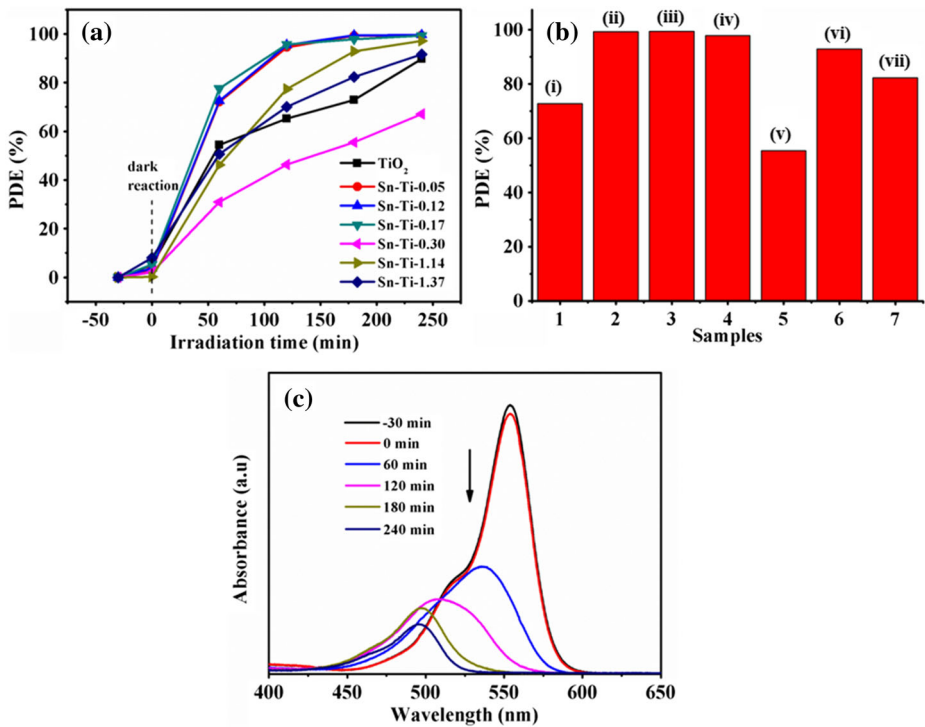


**Fig. 2** **a** PDE of RhB using TiO<sub>2</sub> and Sn-Ti-x samples, **b** comparison diagram of various phases and PDE ((i) TiO<sub>2</sub> (A), (ii) Sn-Ti-0.05 (A), (iii) Sn-Ti-0.12 (A), (iv) Sn-Ti-0.17 (predominant A and minute R), (v) Sn-Ti-0.30 (equal portion of A and R), (vi) Sn-Ti-1.14 (R), Sn-Ti-1.37 (R); where A = anatase and R = rutile phases) and **c** repetitive scan spectra of photocatalytic degradation of RhB with Sn-Ti-0.05 at various irradiation times under visible light in water

work (Fig. 2b). This indicates that the phase transformation is very important role of photocatalytic activity in metal oxide based materials. It is revealing a positive photocatalytic effect under the presence of low level tin and presumably anatase phase, structural defects or oxygen vacancies. It can be concluded that the low level tin doping into the anatase phase of TiO<sub>2</sub> is beneficial for the photocatalytic activity. The characteristic absorption band of RhB at 554 nm diminishes quickly under visible light irradiation (Fig. 2c). Usually, the photocatalysts with high adsorption affinity for the reactant tend to show high photocatalytic activity.

In Fig. 3, the relative area intensity of paramagnetic Sn doped TiO<sub>2</sub> (doublet) sites, magnetic components (sextet 1 and sextet 2), the saturation magnetization ( $M_s$ ) and coercive field ( $H_c$ ) values of bulk magnetism, and the photocatalytic activity PDE were plotted for various x (Sn/Ti (%)). The  $M_s$  and  $H_c$  values published in our previous paper [6] are used herein. The intensity of paramagnetic doublet of Sn<sup>4+</sup> was found to decrease with increasing x; however, opposite behavior was observed for magnetic components. Moreover, when the PDE are compared with the intensity of the paramagnetic doublet, it is likely that paramagnetic Sn species influenced the photocatalytic activity due to the stabilization of the electronic excitation energy level. The higher amounts of structural defects are likely related to the induced magnetism rather than photocatalytic activity. Irregular behavior was observed for Sn-Ti-0.30 sample, which may decrease its photocatalytic activity due

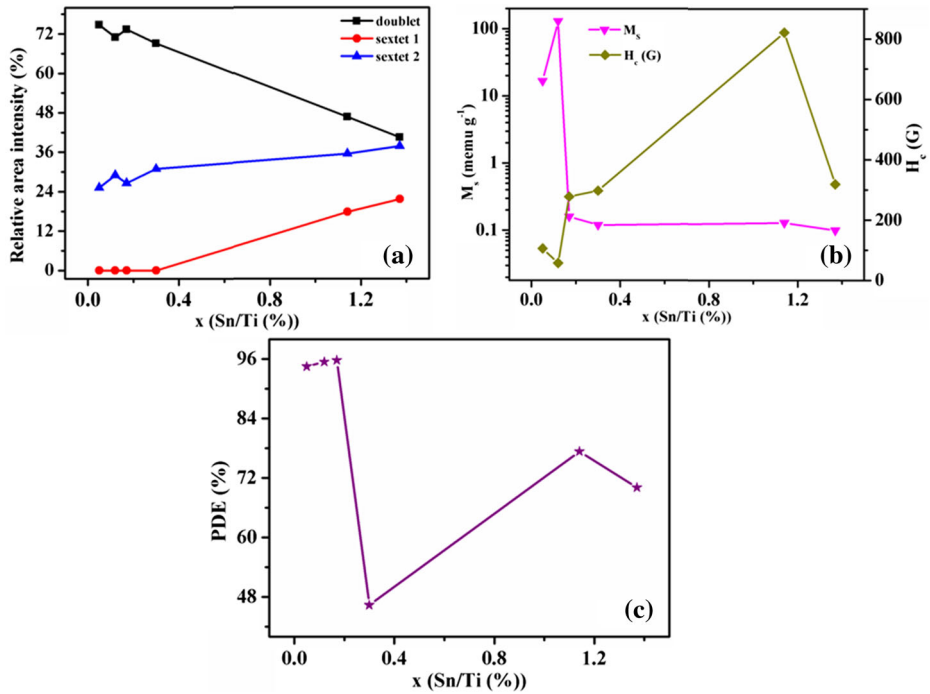


**Fig. 3** Variation of relative area intensity of doublet, sextets 1 and 2 obtained from <sup>119</sup>Sn Mössbauer measurements (a), saturation magnetization ( $M_s$ ) and coercivity ( $H_c$ ) obtained from room temperature vibrating sample magnetometer (VSM) (b) and PDE values (at 120 min) (c) with various atomic ratios ( $x = \text{Sn/Ti} (\%)$ ) of Sn-Ti- $x$  samples

to the inhibition of the carrier transformer between rutile and anatase phases. Furthermore, the very low level Sn doped samples (Sn-Ti-0.05 and Sn-Ti-0.12) showed high magnetism, which might be due to the deformed anatase structure, whereas the high photocatalytic activity was kept because the diluted Sn doping did not affect the anatase phase transformation. The  $H_c$  increased with the increase of doped Sn concentration, which shows that the  $H_c$  may be strongly correlated with the mixed phases and structural defects. It was concluded that the low level Sn doping into anatase TiO<sub>2</sub> stabilizes the electronic excitation energy level and the electron transfer under irradiation, whereas the high level Sn doping induces the mixed phases and magnetic defects at the interfaces.

### 4 Conclusions

Sn-TiO<sub>2</sub> nanocrystals were successfully synthesized by a hydrothermal method. Mössbauer spectra of low level Sn doped TiO<sub>2</sub> samples were decomposed into a doublet and a sextet and Mössbauer spectra of high level Sn doped samples into one more sextet magnetic component. The magnetic fields of the two sextets may indicate different spin arrangement. All Sn-TiO<sub>2</sub> samples showed weak ferromagnetic behavior in this work. In addition, the photocatalytic activities were measured by the degradation of RhB under visible light irradiation and the relation was observed between amount of Sn sites and photocatalytic activity. The

results suggest that small amount of tin content in anatase TiO<sub>2</sub> preferably improved photocatalytic activity due to the more efficient separation of photoinduced electrons and holes on its surface. We observed the relationship between photocatalytic activity and relative area of Sn sites through <sup>119</sup>Sn Mössbauer study. Also, it was concluded that paramagnetic Sn doped sites influence photocatalytic activity primarily due to stabilization of the electronic excitation energy level and the electron transfer under irradiation. It can be concluded that the low level Sn doping into TiO<sub>2</sub> is efficient for the photocatalytic degradation of the sample under study whereas the high level Sn doping induces the phase segregation and the magnetic defects at the interfaces.

**Acknowledgments** This work was supported by National Natural Science Foundation of China (11079036, 21476232), the CAS President's International Fellowship Initiative (PIFI) programme (No. 2016PT023) and International Young Scientists Research Fund project funded by the NSFC (No. 2161101071).

## References

1. Li, X., Xiong, R.C., Wei, G.: Preparation and photocatalytic activity of nanoglued Sn-doped TiO<sub>2</sub>. *J. Hazard. Mater.* **164**, 587–591 (2009)
2. Jiang, H., Xing, J., Chen, Z., Tian, F., Cuan, Q., Gong, X., Yang, H.: Enhancing photocatalytic activity of Sn doped TiO<sub>2</sub> dominated with {1 0 5} facets. *Catal. Today* **225**, 18–23 (2014)
3. Jing, L., Fu, H., Wang, B., Wang, D., Xin, B., Li, S., Sun, J.: Effects of Sn dopant on the photoinduced charge property and photocatalytic activity of TiO<sub>2</sub> nanoparticles. *Appl. Catal. B* **62**, 282–291 (2006)
4. Li, J., Zeng, H.C.: Hollowing Sn-doped TiO<sub>2</sub> nanospheres via Ostwald ripening. *J. Am. Chem. Soc.* **129**, 15839–15847 (2007)
5. Ganeshraja, A.S., Clara, A.S., Rajkumar, K., Wang, Y.J., Wang, Y., Wang, J., Anbalagan, K.: Simple hydrothermal synthesis of metal oxides coupled nanocomposites: structural, optical, magnetic and photocatalytic studies. *Appl. Surf. Sci.* **353**, 553–563 (2015)
6. Ganeshraja, A.S., Thirumurugan, S., Rajkumar, K., Zhu, K., Wang, J., Anbalagan, K.: Effects of structural, optical and ferromagnetic states on the photocatalytic activities of Sn–TiO<sub>2</sub> nanocrystals. *RSC Adv.* **6**, 409–421 (2016)
7. Wang, C., Shao, C., Zhang, X., Liu, Y.: SnO<sub>2</sub> nanostructures–TiO<sub>2</sub> nanofibers heterostructures: controlled fabrication and high photocatalytic properties. *Inorg. Chem.* **48**, 7261–7268 (2009)
8. Fabritchnyi, P.B., Korolenko, M.V., Afanasov, M.I., Danot, M., Janod, E.: Mössbauer characterization of tin dopant ions in the antiferromagnetic ilmenite MnTiO<sub>3</sub>. *Solid State Commun.* **125**, 341–346 (2003)
9. Nomura, K.: Magnetic properties and oxygen defects of dilute metal doped tin oxide based. *Croat. Chem. Acta* **88**, 579–590 (2015)
10. Pan, L., Zou, J.-J., Zhang, X., Wang, L.: Water-mediated promotion of dye sensitization of TiO<sub>2</sub> under visible light. *J. Am. Chem. Soc.* **133**, 10000–10002 (2011)
11. Sun, J., Wang, X.L., Sun, J.Y., Sun, R.X., Sun, S.P., Qiao, L.P.: Photocatalytic degradation and kinetics of Orange G using nano-sized Sn(IV)/TiO<sub>2</sub>/AC photocatalyst. *J. Mol. Catal. A* **260**, 241–246 (2006)